Applied Energy Symposium 2021: Low carbon cities and urban energy systems
September 4-8, 2021, Matsue, Japan
Paper ID: 74

Numerical simulation of the aluminum column-wing type refrigerant-direct radiant cooling system

Tingting Jiang[1], Shijun You[1, 2], Huan Zhang[1, 2], Yaran Wang [1, 2*], Wandong Zheng[1, 2]

1 School of Environmental Science and Engineering, Tianjin University, Jinnan District, Tianjin 300350, PR China

2 Key Laboratory of Efficient Utilization of Low and Medium Grade Energy (Tianjin University), Ministry of Education of China, Tianjin 300350, PR China

ABSTRACT

The refrigerant-direct radiant cooling (RDRC) systems have become increasingly popular owing to good thermal comfort and high energy efficiency. However, the existing RDRC terminal has complex structure and large occupation area. To tackle these problems, an aluminum column-wing type RDRC (ACT-RDRC) terminal is presented. The detailed numerical model is developed to explore the thermal performance of this system and validated with experimental data. Results shows that when the evaporating temperature increases from 6.0 °C to 14.0 °C, the ratio of the natural convection, condensation latent and radiant cooling capacities changes from 4.6:2.1:1 to 4.5:1.4:1, which indicates that the natural convection is a main contributor in the heat transfer process of this system. To meet the thermal comfort requirements, the relative humidity less than 60% is recommended with the indoor air temperature of 28 °C. A characteristic equation is proposed to accurately predict the cooling performance of the ACT-RDRC system, which is conductive to promote its application.

Keywords: refrigerant-direct radiant cooling system; numerical model; cooling performance; thermal comfort; characteristic equation

NONMENCLATURE

Abbreviations	
ACT-RDRC	aluminum column-wing type refrigerant-direct radiant cooling
AUST	comprehensive temperature of the building envelope

Symbols	
A	area (m^2)
b_w	simplified coefficient
c_p	specific heat ($J\cdot kg^{-1}\cdot K^{-1}$)
D	diameter (mm)
G	refrigerant mass flow rate ($kg\cdot s^{-1}$)
h	convective heat transfer coefficient ($W\cdot m^{-2}\cdot K^{-1}$)
h_D	conversion heat release coefficient ($W\cdot m^{-2}\cdot K^{-1}$)
I	enthalpy ($J\cdot kg^{-1}$)
n	number of section
p	pressure (Pa)
Q	cooling capacity (W)
t	temperature (°C)
t_m	mean surface temperature (°C)
W_c	condensation water weight ($kg\cdot s^{-1}$)
x	vapor quality
z	shape parameter of rib
ΔI_a	indoor air excess enthalpy ($J\cdot kg^{-1}$)
Δl	control volume length (m)
Δt_b	surface excess temperature (°C)
Greek Symbols	
λ	thermal conductivity ($W\cdot m^{-1}\cdot K^{-1}$)
ε	emissivity
σ	Stefan-Boltzmann constant, 5.67×10^{-8} $W\cdot m^{-2}\cdot K^{-4}$
φ	relative humidity (%)
Subscripts	
al	aluminum-alloy panel
be	building envelope
coi	inner surface of copper pipe

Selection and peer-review under responsibility of the scientific committee of CUE2021

coo	outer surface of copper pipe
e	evaporate
g	gas
i	node *i*
in	inlet
la	latent heat
n	indoor air
out	outlet
r	refrigerant
rad	radiation
t	total
s	sensible
se	connection segment
sur	surface
wa	water

1. INTRODUCTION

In recent years, nearly 23% of the total energy consumption is attributed to building energy consumption. Heating, ventilation and air conditioning systems account for a large proportion in building energy consumption. Radiant cooling systems are widely applied in many buildings since they have good thermal comfort and high energy efficiency, compared with traditional air conditioning systems.

Many scholars have studied the radiant cooling systems in terms of thermal comfort and energy efficiency. Tian et al. [1] investigated the occupant comfort of the radiant ceiling cooling coupled with overhead dedicated outdoor air system based on the PMV model. The results showed that this system had the ability to provide better comfort conditions in comparison with conventional air conditioning systems. Cen et al. [2] conducted a comparative study of a radiant floor system and a fan coil system through questionnaire survey, and suggested that the former one had great potential to achieve better thermal comfort in various heights space. Wang et al. [3] proposed an energy-efficient radiant cooling system with fresh air supply and explored its energy conserving potentiality, with the result showing that the COP of this system was improved by 25.8% ~ 30.1% compared to conventional systems. A multi-floor radiant slab cooling system was carried out by Kwong et al. [4] to evaluate the energy consumption in a green building in Malaysia, and justified that this system could save 34% of the energy consumption.

The heat transfer characteristics of radiant cooling systems have also attracted more attentions. Xu et al. [5] developed a novel three phase zone numerical model of the capillary floor radiant cooling system, and studied the phase-change heat transfer characteristics, the best water supply temperature and the change rule of the surface temperature of the floor. A three-dimensional finite volume simulation of radiant cooling panel systems was established by Serageldin et al. [6]. The results showed that when the curvature cord length ratio to curvature radius increased from 0 to 2, the radiant heat transfer coefficient was declined by 31% and the convective heat transfer coefficient was improved by 174%. However, the previous studies are mainly focused on radiant cooling systems using chilled water as circulating medium, which requires secondary heat exchange. In the authors' previous work [7], a radiant-convective cooling system with the refrigerant-cooling radiant terminal is proposed, which adopts refrigerant to exchange heat with indoor environment directly and has high energy efficiency. Additionally, this system allows dew condensation behavior on its surface and possesses the capability of independent dehumidification. While the refrigerant-cooling radiant terminal uses steel plate as packaging shell, and its structure was complex and requires a large installation area.

To simplify the equipment, the ACT-RDRC terminal is presented. The numerical model of this terminal is established and validated with experimental data. Based on the numerical model, the thermal performance of the ACT-RDRC system is investigated. A characteristic equation for type-select calculation of this system is put forward, which can provide reference for engineering application.

2. METHODOLOGY

2.1 Physical model

The schematic of the ACT-RDRC terminal is depicted in Fig. 1, with the dimension of 1600 mm (L) × 100 mm (W) × 650 mm (H). The key components are two aluminum-alloy-column panels, four branches copper pipes, cold-storage medium (water), many rectangular fins and one condensation collection plate. The S-shape copper pipes filled with refrigerant are embedded in the aluminum-alloy columns. Water is adopted as the cold-storage medium and sandwiched between copper pipes and aluminum-alloy columns to enhance the heat capacity. The rectangular fins are evenly arranged on the backside of the front panel and both sides of the back panel. The condensation collection plate is located at the bottom to collect condensation water. During the operating period, the heat from the indoor environment is transferred to the ACT-RDRC terminal surface and fins

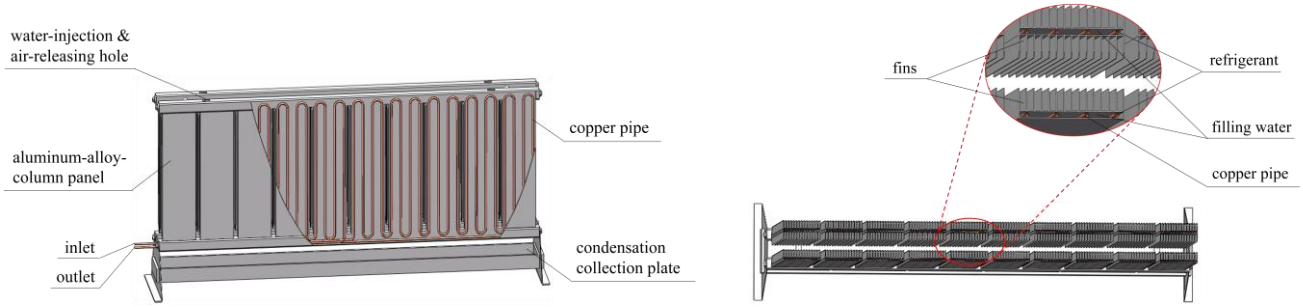

(a) front (b) profile

Fig 1 The schematic of the ACT-RDRC terminal.

through natural convection and radiation, and then delivered to the water and copper pipes via heat conduction. Finally, the heat is released to the refrigerant through convection.

2.2 Numerical model

The following assumptions are considered to establish the numerical model:

(1) The heat transfer process of the ACT-RDRC terminal is considered as one-dimensional and steady-state;

(2)The ACT-RDRC terminal is made up of a series of parallel concentric sleeves;

(3) The heat conduction losses occur in the axial-direction of the refrigerant, copper pipes, water and aluminum-alloy panels are ignored;

(4) The water in the aluminum-alloy columns is stationary;

(5) The indoor air temperature and exterior wall temperature remain constant.

Fig. 2 shows the control volume of each component of the ACT-RDRC terminal, which are divided into *n* sections along the refrigerant flow direction with the length of Δl. The temperatures of the refrigerant, inner and outer surface of the copper pipes, water and aluminum-alloy panel are defined as t_r, t_{coi}, t_{coo}, t_{wa}, t_{al}, respectively. Based on the finite volume method, the governing equations for *i* th node are given as follows:

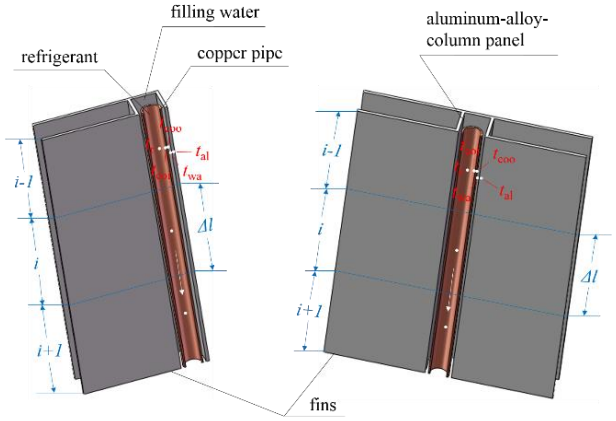

Fig 2 Sketch of control volumes of the ACT-RDRC terminal.

For the refrigerant:

$$G[I_{\text{r-in}}(i)-I_{\text{r-out}}(i)]+\pi D_{\text{r}}\Delta l\cdot h_{\text{r-coi}}[t_{\text{coi}}(i)-t_{\text{r}}(i)]=0,\quad 0<x(i)<1 \tag{1}$$

$$c_{pg}(i)G[t_{\text{r-in}}(i)-t_{\text{r-out}}(i)]+\pi D_{\text{r}}\Delta l\cdot h_{\text{r-coi}}(i)[t_{\text{coi}}(i)-\frac{t_{\text{r-in}}(i)+t_{\text{r-out}}(i)}{2}]=0,\quad x(i)=1 \tag{2}$$

$$I_{\text{r}}(i)=x(i)\cdot I_{\text{rl}}(i)+[1-x(i)]\cdot I_{\text{rg}}(i) \tag{3}$$

For the inner surface of the copper pipe:

$$\pi D_{\text{r}}\Delta l\cdot h_{\text{r-coi}}(i)[t_{\text{r}}(i)-t_{coi}(i)]+\frac{t_{\text{coo}}(i)-t_{\text{coi}}(i)}{\frac{1}{2\pi\lambda_{\text{coi}}}\ln\frac{D_{\text{coo}}}{D_{\text{r}}}}\cdot\Delta l=0,\quad 0<x(i)<1 \tag{4}$$

$$\pi D_{\text{r}}\Delta l\cdot h_{\text{r-coi}}(i)[\frac{t_{\text{r-in}}(i)+t_{\text{r-out}}(i)}{2}-t_{\text{coi}}(i)]+\frac{t_{\text{coo}}(i)-t_{\text{coi}}(i)}{\frac{1}{2\pi\lambda_{\text{coi}}}\ln\frac{D_{\text{coo}}}{D_{\text{r}}}}\cdot\Delta l=0,\ x(i)=1 \tag{5}$$

For the outer surface of the copper pipe:

$$\frac{t_{\text{coi}}(i)-t_{\text{coo}}(i)}{\frac{1}{2\pi\lambda_{\text{coi}}}\ln\frac{D_{\text{coo}}}{D_{\text{r}}}}\cdot\Delta l+\frac{t_{\text{wa}}(i)-t_{\text{coo}}(i)}{\frac{1}{2\pi\lambda_{\text{wa}}}\ln\frac{D_{\text{wa}}}{D_{\text{coo}}}}\cdot\Delta l=0 \tag{6}$$

For the water:

$$\frac{t_{\text{coo}}(i)-t_{\text{wa}}(i)}{\frac{1}{2\pi\lambda_{\text{wa}}}\ln\frac{D_{\text{wa}}}{D_{\text{coo}}}}\cdot\Delta l+\frac{t_{\text{al}}(i)-t_{\text{wa}}(i)}{\frac{1}{2\pi\lambda_{\text{al}}}\ln\frac{D_{\text{al}}}{D_{\text{wa}}}}\cdot\Delta l=0 \tag{7}$$

For the aluminum-alloy panel:

$$\frac{t_{\text{wa}}(i)-t_{\text{al}}(i)}{\frac{1}{2\pi\lambda_{\text{al}}}\ln\frac{D_{\text{al}}}{D_{\text{wa}}}}\cdot\Delta l+Q_{\text{rad,al-be}}(i)+\frac{h_{\text{air}}(i)}{c_{p\text{-air}}}[I_{\text{air}}-I_{\text{al}}(i)]\cdot(\pi D_{\text{al}}\Delta l+w_{\text{se}}\Delta l\cdot 2)+\frac{2h_D(I_{\text{air}}-I_{\text{rib}})}{b_w}\cdot\frac{th(z\Delta l)}{z}\cdot 2=0 \tag{8}$$

$$Q_{\text{rad,al-be}}=\varepsilon\cdot\sigma\cdot A_{\text{al}}[(t_{\text{m}}+273.15)^4-(AUST+273.15)^4] \tag{9}$$

$$AUST=\frac{\sum_{i=1}^{n}A_i t_i}{\sum_{i=1}^{n}A_i} \tag{10}$$

Therein, the correlations of $h_{r\text{-}coi}$, h_{air} and h_D of the numerical model can be derived from Ref. [8].

2.3 Solution strategy

The flowchart of the solution strategy is shown in Fig. 3. The calculation steps are as follow: (a) Input operating parameters and assume initial value of the ACT-RDRC terminal surface temperature t'_{al}; (b) Calculate the total cooling capacity of the ACT-RDRC system $Q_{t,i}$ and then determine the flow state of the refrigerant x_i; (c) Calculate the convective heat transfer coefficient $h_{r\text{-}coi,i}$ and the value of $t_{al,i}$ by iterative method until the convergence condition is satisfied; (d) Output all values of t_r, t_{coi}, t_{coo}, t_{wa} and t_{al} until i=n.

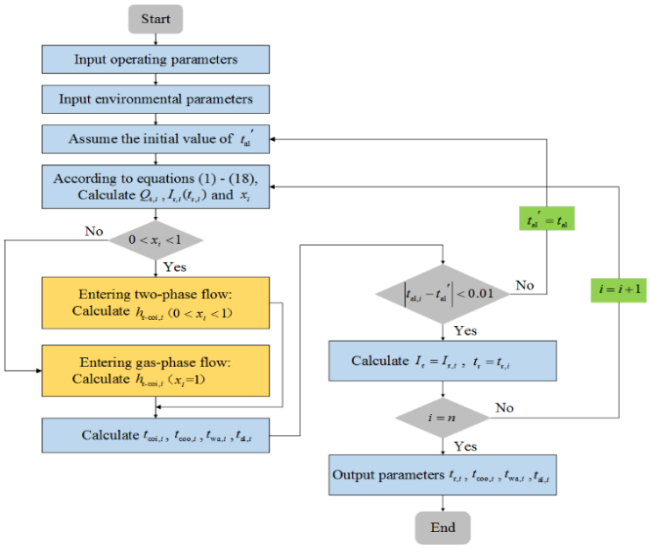

Fig 3 Flowchart of the solution strategy.

3. TEST RIG

3.1 System description

In order to validate the accuracy of the numerical model of the ACT-RDRC terminal, the experiments are carried out in a calorimetric room, as shown in Fig. 4. It consists of indoor-environmental chamber and outdoor-environmental chamber, and their thermal environments are regulated by independent air conditioning systems. A test room is constructed in the indoor-environmental chamber to avoid forced air convection. The ACT-RDRC system is composed of compressor, gas-liquid separator, four-way valve, condenser, sub-cooler, electronic expansion valve and the ACT-RDRC terminal (evaporator). In the experiments, the temperature of the test room is controlled at 26 °C ~ 30 °C, and the relative humidity is set at 60%. The evaporating temperature of the ACT-RDRC system is maintained at 6.0 °C ~ 12.0 °C. The inlet and outlet temperatures and pressures of the ACT-RDRC terminal and condenser, refrigerant mass flow rate, indoor air temperature, relative humidity and the ACT-RDRC terminal surface temperature are recorded.

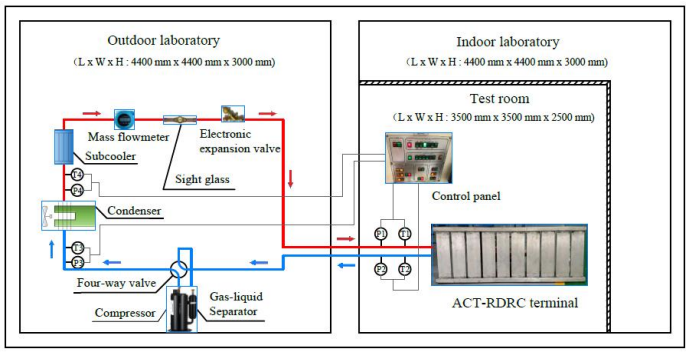

Fig 4 Schematic diagram of the ACT-RDRC system.

3.2 Model validation

The simulated results and experimental data of the ACT-RDRC system are shown in Fig. 5. As is shown that the simulated results have good match with the measured data, and the relative errors of the refrigerant outlet temperature and pressure, mean surface temperature of the ACT-RDRC terminal and the total cooling capacity are 2.4% ~ 8.2%, 2.1% ~ 3.1%, 3.5% ~ 8.7% and 1.5% ~ 6.7%, respectively. Therefore, the established numerical model is reliable and can accurately evaluate the thermal performance of the ACT-RDRC system.

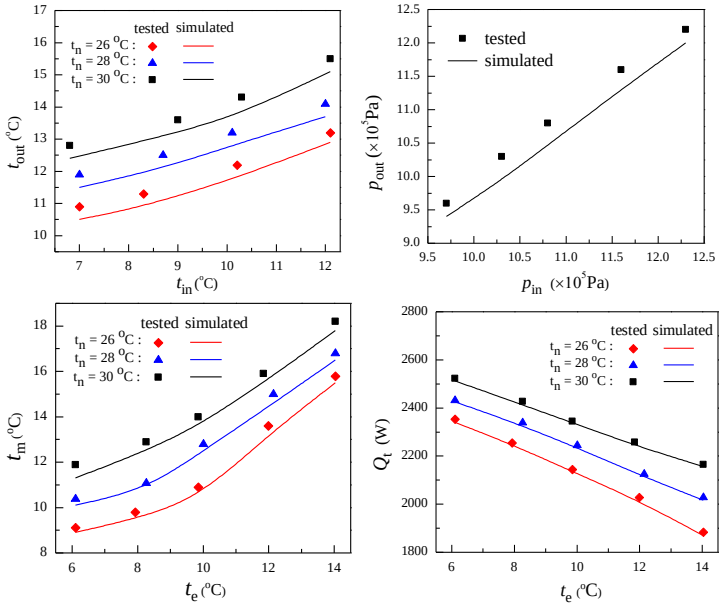

Fig 5 Comparison of simulated results and measured data.

4. RESULTS AND DISCUSSION

4.1 Cooling performance analysis

The variation trend of the cooling capacity of the ACT-RDRC system with the evaporating temperature is depicted in Fig. 6, under the indoor air temperature of 26 °C and relative humidity of 60%. With the evaporating temperature increases from 6.0 °C to 14.0 °C, the total cooling capacity is reduced from 1443.9 W to 1183.3 W due to the decrease of the refrigerant evaporation rate and the weakness of heat exchange intensity. Besides, both the sensible and radiant cooling capacities are declined, which is ascribed that the mean surface temperature of the ACT-RDRC terminal ascends, leading to the depression of the natural convective and radiant heat transfer between the ACT-RDRC terminal and indoor environment. Moreover, the latent cooling capacity drops from 394.4 W to 229.7 W with the rise of the evaporating temperature. It can be attributed that the dehumidifying performance mitigates, resulting in the diminution of the condensation water quality. Furthermore, the ratio of natural convection, condensation latent and radiant cooling capacities changes from 4.6:2.1:1 to 4.5:1.4:1, which indicates that the natural convective heat transfer is a major factor of the total cooling capacity. It can be concluded that the rectangular fins attached to the ACT-RDRC terminal exert significant role in promoting the natural convective heat transfer.

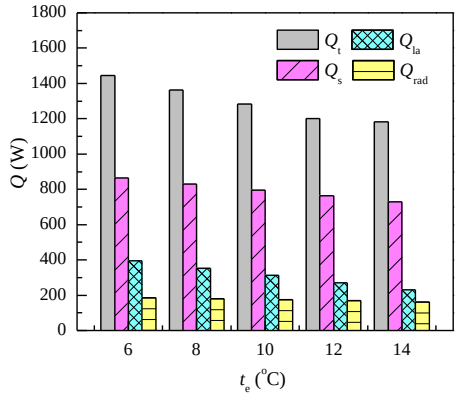

Fig 6 Effect of evaporating temperature on cooling capacity.

4.2 *Indoor thermal comfort*

The relative humidity is a crucial indicator affecting human thermal sensation. However, the ASHRAE standard does not stipulate the humidity limitation regarding to thermal comfort at present. The effects of the relative humidity on condensation water weight and PMV value with the indoor air temperature of 28 °C are illustrated in Fig 7. As the relative humidity increases from 40% to 70%, the condensation water weight increases from 1.85×10^{-5} kg s^{-1} to 26.7×10^{-5} kg s^{-1}. This phenomenon can be explained that the surface temperature of the ACT-RDRC terminal is lower than the dew point temperature of indoor air consistently, and then the generation rate of condensation water grows up. It indicates that the ACT-RDRC system exhibits excellent dehumidifying performance. In addition, the PMV value is ascended from 0.42 to 0.88 with the rise of the relative humidity. According to ASHRAE Standard [9], when the relative humidity increases from 40% ~ 46%, the thermal comfort level of the ACT-RDRC system attains Class B. Correspondingly, when the relative humidity is less than 60%, the thermal comfort level can meet Class C. Therefore, it is advisable to set the relative humidity not exceed 60% to guarantee the comfortable indoor thermal environment.

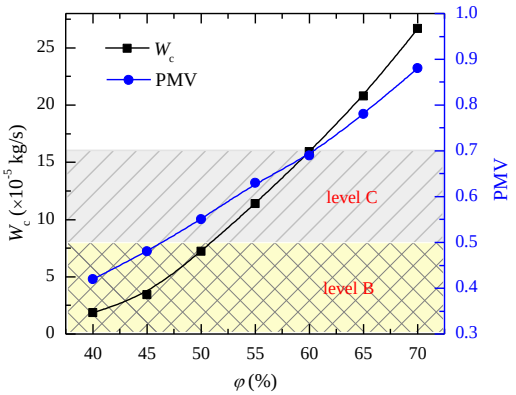

Fig 7 Effect of relative humidity on condensation water weight and PMV value.

4.3 *Characteristic equation*

As the existing characteristic equation is only used for radiant cooling system with chilled water [10], in order to facilitate the type-select calculation of the ACT-RDRC terminal, a characteristic equation is proposed to evaluate the relationship between cooling capacity and four parameters: indoor air enthalpy, the enthalpy of saturated boundary layer on the ACT-RDRC terminal surface, evaporating temperature and the comprehensive temperature of building envelope (AUST). The simulated results of this system under different operating conditions are described in Table 1.

Table 1. The simulated results of the ACT-RDRC system.

Case	t_n (°C)	φ (%)	t_e (°C)	t_m (°C)	AUST (°C)	Q_t (W)
1	26.0	60.0	11.9	17.0	25.9	863.6
2	26.0	60.0	10.0	16.1	25.8	1062.2
3	26.0	60.0	7.7	14.6	25.8	1425.8
4	20.0	81.0	7.7	12.3	19.9	1157.6
5	24.0	63.5	7.7	13.5	23.8	1322.3
6	28.0	50.0	7.7	14.9	27.8	1425.6
7	30.0	44.6	7.7	15.8	29.8	1450.9

8	26.0	40.0	7.7	12.4	25.8	1182.1
9	26.0	50.0	7.7	13.5	25.8	1318.7
10	26.0	60.0	7.7	14.7	25.8	1411.1
11	26.0	70.0	7.7	16.0	25.8	1455.9
12	30.0	40.0	7.7	14.9	29.8	1425.9
13	30.0	50.0	7.7	16.7	29.8	1470.8
14	30.0	60.0	7.6	18.5	29.8	1498.2
15	30.0	70.0	7.6	20.2	29.8	1524.2

The indoor air excess enthalpy is defined as:

$$\Delta I_a = I_{\mathrm{n}} - I_{\mathrm{sur}} \tag{11}$$

The surface excess temperature is considered as:

$$\Delta t_b = AUST - t_{\mathrm{e}} \tag{12}$$

Based on the simulated results, the characteristic equation of the ACT-RDRC system can be fitted by least square method, as follows:

$$Q_{\mathrm{t}} = 235.98 \Delta I_a^{\,0.824} \Delta t_b^{\,0.332} \tag{13}$$

where the coefficient of determination is 0.98.

In these cases, the ranges of indoor air temperature, relative humidity, the ACT-RDRC terminal surface temperature, AUST and evaporating temperature are 20 ^{o}C ~ 30 ^{o}C, 40% ~ 81%, 12.3 ^{o}C ~ 20.2 ^{o}C, 19.9 ^{o}C ~ 29.8 ^{o}C and 7.6 ^{o}C ~ 11.9 ^{o}C, respectively. Therefore, the characteristic equation of the ACT-RDRC system can be used in this scope and is conductive to provide reference for engineering application.

5. CONCLUSIONS

In this paper, a numerical model of the ACT-RDRC terminal is established and validated with the experimental data. Based on the numerical model, the thermal performance of the ACT-RDRC system is investigated. The following conclusions are drawn:

(1) The numerical model of the ACT-RDRC terminal shows satisfactory agreement with the measured data and can accurately predict the thermal performance of this system.

(2) In the ACT-RDRC system, the natural convective heat transfer exerts a significant role in total cooling capacity. Besides, this system has obvious superiority in independent dehumidification.

(3) When the indoor air temperature remains 28 ^{o}C and relative humidity keeps below 60%, the ACT-RDRC system can provide comfortable indoor thermal environment. The proposed characteristic equation is beneficial for type-select calculation of the ACT-RDRC terminal in engineering application.

ACKNOWLEDGEMENT

This work was supported by the National Natural Science Foundation of China (No. 52008290).

REFERENCE

[1] Z. Tian, L. Yang, X. Wu, Z. Guan, A field study of occupant thermal comfort with radiant ceiling cooling and overhead air distribution system, Energy and Buildings, 223 (2020) 109949.

[2] C. Cen, Y. Jia, K. Liu, R. Geng, Experimental comparison of thermal comfort during cooling with a fan coil system and radiant floor system at varying space heights, Building and Environment, 141 (2018) 71-79.

[3] Y. Wang, Y. Yin, X. Zhang, X. Jin, Study of an integrated radiant heating/cooling system with fresh air supply for household utilization, Building and Environment, 165 (2019) 106404.

[4] Q.J. Kwong, S.J. Kho, J. Abdullah, V.R. Raghavan, Evaluation of energy conservation potential and complete cost-benefit analysis of the slab-integrated radiant cooling system: A Malaysian case study, Energy and Buildings, 138 (2017) 165-174.

[5] Y. Xu, B.B. Sun, L.J. Liu, X.Y. Liu, The numerical simulation of radiant floor cooling and heating system with double phase change energy storage and the thermal performance, Journal of Energy Storage, 40 (2021) 102635.

[6] A.A. Serageldin, M. Ye, A. Radwan, H. Sato, K. Nagano, Numerical investigation of the thermal performance of a radiant ceiling cooling panel with segmented concave surfaces, Journal of Building Engineering, 42 (2021) 102450.

[7] T. Jiang, S. You, H. Zhang, S. Wei, H. Liu, Y. Wang, Experimental study and thermo-economic analysis of a novel radiant-convective cooling system, International Journal of Refrigeration, 2021.

[8] T. Jiang, S. You, Z. Wu, H. Zhang, Y. Wang, S. Wei, Performance analysis of the refrigerant-cooling radiant terminal: A numerical simulation, Applied Thermal Engineering, 197 (2021) 117395.

[9] P.O. Fanger, Thermal comfort, Danish Technical Press, Copenhagen, 1970.

[10] JG/T 403-2013, Test Methods for Thermal Performance of Radiant Cooling and Heating Unit, Standards Press of China, Beijing, 2013.